Effects of catalyst layer on the structural change of a membrane electrode assembly under humidity cycle tests

Yoshiyuki Hashimasa*, Tomoaki Numata, Noboru Yoshimura

FC-EV Research Division, Japan Automobile Research Institute, 2530 Karima, Tsukuba, Ibaraki 305-0822, Japan

HIGHLIGHTS

- We examined effects of catalyst layer on the structural change of an MEA.
- Swelling deformation becomes small by enlarging the catalyst layer thickness. Decrease of storage elastic modulus of MEA was prevented by the catalyst layer.
- Catalyst layer reduce the structural change of an MEA under the humidity cycle test.

ARTICLE INFO

ABSTRACT

Structural changes in a polymer electrolyte membrane (PEM) and a membrane electrode assembly (MEA) of different catalyst thickness under humidity cycle tests were investigated. Nafion211 membrane was used in this study. The catalyst layer thickness of MEAs was set to $2-10$ μm using catalyst paste of the same composition. Dimensional changes in the PEM and MEA due to swelling were measured, and dynamic mechanical analysis (DMA) of the membrane and MEA were carried out. Moreover, humidity cycle tests for the MEA were carried out according to the conditions specified in the FCCJ protocol, and structural changes in the MEA after the tests were examined. It was shown that the membranous structural change under humidity cycle tests tends to become small when the thickness of the catalyst layer is large.

© 2014 Elsevier B.V. All rights reserved.

1. Introduction

With growing public interest in environmental protection and energies other than oil, research and development is under way on polymer electrolyte fuel cells (PEFCs) as a substitute for the internal combustion engine. Improved durability and cost reduction of fuel cell stacks are two important issues to enable widespread use of fuel cell vehicles. Polymer electrolyte membrane fuel cells, especially for automotive applications, must operate over a wide range of conditions. The Fuel Cell Commercialization Conference of Japan (FCCJ) proposed several methodologies for testing MEAs and their materials [1–5]. We have applied the protocols of FCCJ to standard materials and verified their validity using a JARI standard single cell [6,7]. The JARI standard single cell has an electrode surface area of 25 cm^2 and one serpentine flow channel in each separator of anode and cathode [6]. This cell has a large gas flow rate in a channel, and

is characterized by being easy to produce a pressure distribution. The JARI standard single cell is suitable for simulating the phenomena that may actually occur in a PEFC stack, and so is suitable for material evaluation under conditions near the operating condition of an actual stack. Humidity cycle tests that simulate the operation of a fuel cell vehicle are widely used to test the mechanical durability of a membrane in the form of membrane electrode assemblies (MEAs). In perfluorosulfonic acid membranes, sufficient membrane hydration contributes to good proton conduction. The membrane swells through the absorption of water produced by an electrochemical reaction. Conversely, the membrane shrinks via desorption of water in low-humidity fuel cell operation. The membrane swells and shrinks repeatedly according to the fuel cell environment, which changes with the automotive operating conditions. As a result, the repeated expansion and shrinkage affects the deformation of the polymer electrolyte membrane and decreases its mechanical durability. The humidity cycle test is a means of accelerating mechanical degradation of the membrane, which is an important subject for researchers studying the mechanical behavior of electrolyte membranes. Many

* Corresponding author. Tel.: +81 29 856 0818; fax: +81 29 856 1169.
E-mail addresses: yhashi@jari.or.jp (Y. Hashimasa), tnuma@jari.or.jp (T. Numata), ynoboru@jari.or.jp (N. Yoshimura).

researchers have studied the mechanical behavior of fuel cell membranes under conditions of cycling humidity using numerical models. Compressive, plastic deformation occurs during hygro-thermal loading, resulting in tensile residual stress after unloading [8]. These residual in-plane stresses are the major stress component in the membrane [9,10]. The simulation results of in situ fuel cell hygro-thermal cycling in a simplified two-dimensional fuel cell model supports the theory of hygro-thermal driven mechanical stress causing the formation of pinholes in the channel [11]. Humidity cycling leads to mechanical failure of the membrane due to in-plane swelling strain where the fastening force is lower within the channel portions of grooved gas flow fields. A methodology to predict the durability of PEM under humidity cycling was presented, and such testing can be used to evaluate membrane failure [12]. Mechanical stress in the membrane is caused by the restriction of its swelling by the gas diffusion layer (GDL) and cell assembly, both of which influence the compressive stress distribution [13–15]. From the results of research on MEA wrinkle deformation, caused by compressive stress along with in-plane swelling as an initial phase of the degradation, a lower swelling ratio in the in-plane direction and a thicker membrane prevent membrane buckling [16]. Most of the above-mentioned literature investigated the effects of fastening force distribution caused by the gas flow field configuration or by imperfect geometry of the GDL surface [17]. The effects of the MEA catalyst layer have not been sufficiently discussed. In this study, we experimentally investigated the effects of the catalyst layer on the swelling characteristics, thermal deformation behavior, and structural change of a membrane electrode assembly under humidity cycle tests.

2. Experimental

2.1. MEA preparation

MEAs were prepared using a commercial Pt/C catalyst (TEC10E50E), polymer dispersion (DE2020) and polymer electrolyte membrane (NR211). The catalyst paste was applied onto a Teflon sheet using the doctor-blade method and was heat-treated at 125 °C for 1 h. The weight ratio of electrolyte polymer to carbon support in the paste was 1.0. The Pt metal loading was calculated based on the chemical composition of the catalyst paste. A sheet of electrolyte membrane (8 × 8 cm) was sandwiched between catalyst sheets of 25 cm² (5 × 5 cm), with the catalyst layer side of the sheets in contact with the membrane. The sheet-membrane unit was hot-pressed at 135 °C for 10 min, after which the Teflon sheets were removed to obtain an MEA. The thickness of the catalyst layers of an MEA anode and cathode was set at 2–10 μm at the same time. The composition of the catalyst layer was the same regardless of the thickness of the catalyst layer, and the thickness of the catalyst layer was adjusted by varying the clearance gap of the blade. That is, a catalyst layer with larger thickness had a greater Pt loading. MEA specifications as prepared in this study are shown in Table 1.

Table 1
MEA specifications.

Catalyst	Pt/CB (TEC10E50E), TKK
Thickness of anode/cathode catalyst layer (anode/cathode Pt loading mg cm^{-2})	0/0 μm (without catalyst layer)
	2/2 μm (0.05/0.05)
	10/10 μm (0.3/0.3)
Ionomer	D2020, Dupont
I/C	1
Electrolyte membrane	NR211, Dupont
GDL	SGL 24-BCH

2.2. Measurement of dimensional changes in the MEA

We investigated the effects of the thickness of the catalyst layers of an MEA on the deformation characteristics of the membrane by water absorption swelling. Dimensional changes in the PEM and MEA due to swelling were measured. The PEM sample before swelling was cut into a 5-cm square from a PEM sheet. The MEA sample before swelling was cut into a 5-cm square from the electrode area of the MEA prepared by the method described in 2.1 above. The dimensions of the samples before swelling (initial value) were measured at 23 °C and 50% RH. The samples were soaked in deionized water at 80 °C for 1 h, and then the dimensions after swelling were measured. The dimensions along the in-plane direction of the membrane were measured by ruler with a minimum scale value of 0.5 mm. The dimensions along the transverse direction of the membrane were measured by micrometer. From the measurement results, the swelling ratio was calculated by:

$$\text{Swelling ratio} = (X1 - X0)/X0 \times 100\% \qquad (1)$$

x, y: in-plane direction of membrane; z: transverse direction of membrane
0: before swelling; 1: after swelling

2.3. Dynamic mechanical analysis of PEM and MEA

We investigated the effects of the thickness of the catalyst layers of an MEA on the deformation characteristics of the membrane by repeated loading. As for the measurement of physical properties relevant to the glass transition point and tensile strength of an MEA, dynamic mechanical analysis (DMA) of the membrane and the MEA was carried out. The PEM sample was cut into a 50 × 5 mm square from a PEM sheet. The MEA sample was cut into the same size as the PEM from the electrode area of the MEA. The dimensions of the samples before DMA were measured at 23 °C and 50% RH. The samples were soaked at 23 °C and 50% RH for 24 h. The conditions of DMA in this study are shown in Table 2.

2.4. Humidity cycle tests

The deformation by swelling test and the storage elastic modulus in DMA analysis may influence the mechanical durability of the membrane in a humidity cycle test. In order to investigate the effect of the catalyst layer thickness on the mechanical durability of a membrane in the humidity cycle tests under fuel cell operation, the humidity cycle tests proposed by FCCJ were carried out in the form of membrane electrode assemblies (MEAs). Testing was done on a JARI standard single cell, the specifications of which are shown in Table 3.

Table 2
Measurement conditions of dynamic mechanical analyzer.

Sample size	50 × 5 mm
Testing equipment	DMS6100 Dynamic Mechanical Analyzer (Hitachi High-Tech Science Corporation)
Temperature span	−70 °C–200 °C
Rate of temperature increase	2 °C min^{-1}
Frequency	10 Hz
Initial tensile force	50 mN
Measurement mode	Tensile
Distance between chucks	25 mm
Nitrogen flow rate	300 mL min^{-1}
Target distortion	25 μm
Atmospheric gas	Nitrogen flow 300 mL min^{-1}

Table 3
Specifications of JARI standard single cell.

Electrode area	25 cm^2
Number of flow channels, configuration	1, serpentine
Flow channel, land width	1 mm, 1 mm
Flow channel depth	1 mm
Gas flow direction	Counter flow

Table 5
Measurement conditions of linear sweep voltammetry.

Cell temperature	80 °C
Hydrogen flow rate (anode)	200 mL min^{-1}
Nitrogen flow rate (cathode)	200 mL min^{-1}
Anode/cathode relative humidity	100% RH
Scan range	0.05–0.5 V vs. RHE
Scan rate	1 mV s^{-1}

As a general practice, fuel cells undergo an initial break-in operation, because the electrolyte membrane and the electrolyte component in the MEA catalyst layer must be fully humidified to obtain the highest possible performance of the MEA. Newly assembled single cells are considered to suffer low moisture content in their electrolyte elements. In the present study, initial break-in was conducted on MEAs under the conditions of cell temperature of 80 °C and current density of 1000 mA cm^{-2}. The utilization ratio of hydrogen and air was set at 70% and 40%, respectively. Initial break-in was conducted until the cell voltage variation rate declined to less than 2 mV h^{-1}.

Linear sweep voltammetry was used to measure the hydrogen crossover rate through the polymer electrolyte membrane as a diagnostic of the degradation status of the membrane in the humidity cycle tests. Humidity cycle tests using a rectangular waveform of 0–150% RH (4 min cycle^{-1}) were carried out as the membrane mechanical durability test. The test conditions are shown in Table 4.

The tests were terminated when the hydrogen crossover rate through the membrane reached approximately 10 times the initial value. The LSV measurement conditions are summarized in Table 5.

2.5. SEM observation of MEA after humidity cycle tests

Structural changes in the MEA after the humidity cycle tests were examined and then confirmed by scanning electron microscopy (SEM) observation of cross sections in the upper and lower positions of the cell. Hydrogen fuel and air for oxidant gas were supplied to a JARI standard single cell so that they flowed in opposite directions through the MEA. The upper part on the cathode side served as the air inlet and the upper part on the anode side served as the hydrogen outlet. Nitrogen gas in a humidity cycle test was supplied to the cell by the same method.

3. Results and discussion

3.1. Measurement of dimensional changes in the MEA

Strain calculated from the sample size before and after a swelling test is shown in Fig. 1. The direction of one arbitrary side of a square sample is denoted as the x direction, the direction perpendicular to the x direction is the y direction, and the membranous thickness direction is the z direction. Three kinds of samples were prepared for the swelling test: membrane that does not form a catalyst layer, MEA that forms 10 μm catalyst layers with Pt loading of 0.3 mg cm^{-2} on both sides, and MEA that forms 2 μm catalyst layers with Pt loading of 0.05 mg cm^{-2} on both sides. From

Table 4
Conditions of humidity cycle test.

Cell temperature	80 °C
Relative humidity	0% RH (2 min)–150% RH (2 min)
Gaseous species	Nitrogen (on both sides)
Nitrogen flow rate	0.8 SLPM
Pressure	Ambient (no backpressure)
Atmospheric gas	Nitrogen flow 300 mL min^{-1}

the swelling test results, the membrane strain in the x, y, and z directions was larger than that of the MEAs in which the catalyst layers were formed, and the membranous volume swelling rate decreased as a catalyst layer was formed. When the strain was compared in the MEAs with the catalyst layer, it was confirmed that the strain with a thicker (10 μm) catalyst layer was less than that with a thinner (2 μm) catalyst layer in the membrane direction. It is thought that the tensile strength of the MEA increased as a catalyst layer formed on both sides of the membrane.

3.2. Dynamic mechanical analysis of PEM and MEA

Dynamic mechanical analysis (DMA) was carried out to investigate the effects of the formation of a catalyst layer on the
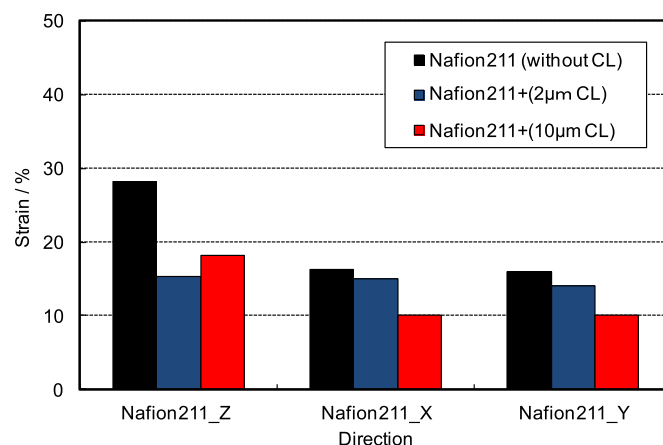

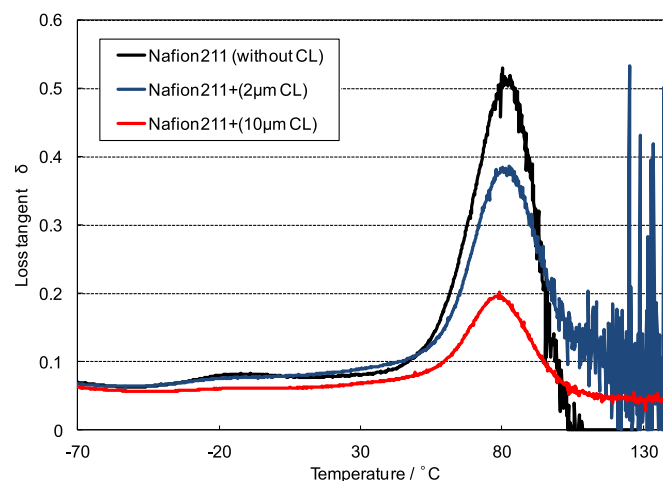**Fig. 1.** Effects of thickness of the catalyst layer on the strain in the swelling test.

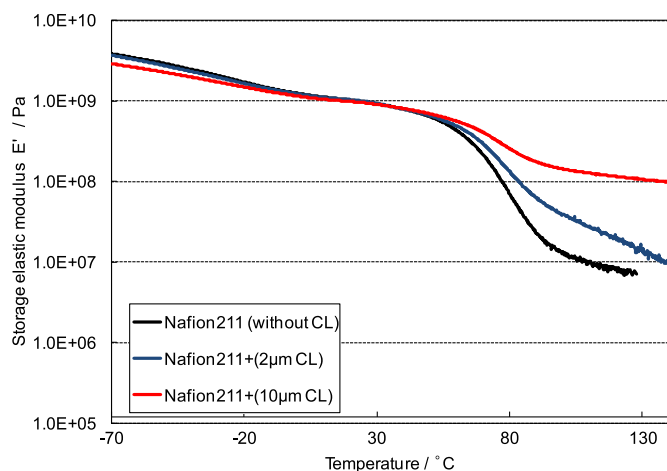**Fig. 2.** Relationship between temperature and loss tangent.

Fig. 3. Effects of thickness of the catalyst layer on the storage elastic modulus.

Fig. 5. Cross-sectional SEM images of the MEA buckling in the upper part of the cell after the humidity cycle tests (anode/cathode catalyst layer thickness: 2/2 μm).

membrane mechanical properties. Fig. 2 shows the relationship between temperature and loss tangent of the membrane and MEA obtained by DMA analysis. Since the loss tangent of each sample peaked at almost the same temperature, it is considered that the formation of a catalyst layer on the membrane did not influence the heat characteristics of the membrane. Hence, the difference in strain between the samples in the swelling test was not affected by the heat characteristics of the samples. Fig. 3 shows the effects of the catalyst layer thickness on the storage elastic modulus of the MEA. This figure shows that the decrease in the storage elastic modulus of MEA in the high-temperature region was prevented when the thickness of the catalyst layer on the membrane was increased. That is, as a characteristic of storage elastic modulus, the membranous stiffness property was improved by the formation of a catalyst layer on both sides of the membrane. This may be one reason for the inhibition of dimensional change in the swelling test.

3.3. Humidity cycle tests

Fig. 4 shows the relationship between the number of cycles in the humidity cycle tests and the normalized cross leakage current with the initial value set to 1. The test results obtained from the MEA for which the thickness of the anode and cathode catalyst layers was set at 2 and 10 μm are shown together. When the number of humidity cycles exceeded 10,000, the cross leakage current increased in both MEAs. Comparing the two MEAs with
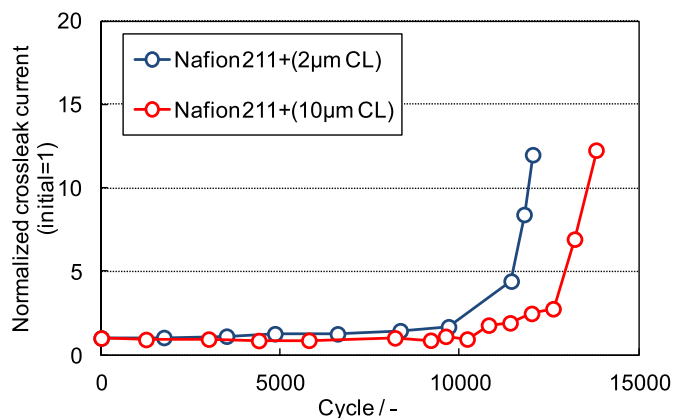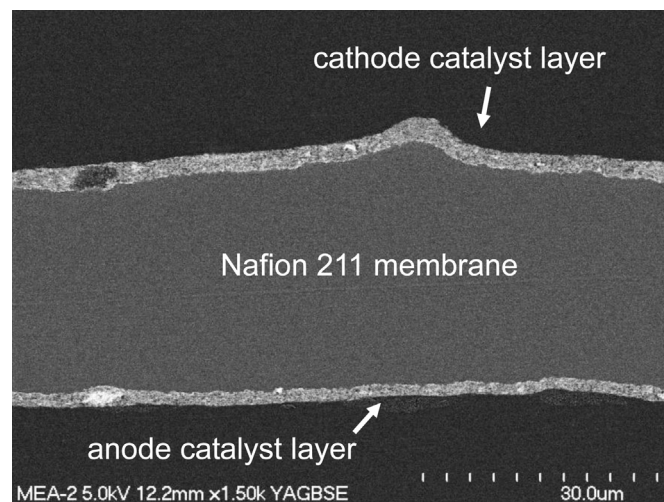
different thickness of catalyst layer, the cross leakage current of the MEA with 2 μm catalyst layer increased until it reached the equivalent value as that of the MEA with 10 μm catalyst layer in fewer cycles. Although the effect was restrictive, the mechanical durability of the membrane in humidity cycle tests was improved by a thicker catalyst layer. We would like to investigate the influence of other test conditions, such as the flow rate of nitrogen gas, and the influence of the structure of a cell. It is necessary to check the reproducibility of the effect of catalyst layer thickness and to examine catalyst layers of different thicknesses in the future.

3.4. SEM observation of MEAs after humidity cycle tests

SEM observation was carried out in order to investigate the structural changes in the MEA after the humidity cycle tests. The structure of the MEA in the upper part of the cell, in which the thickness of the catalyst layer was set to 2 μm at both electrodes, is shown in Fig. 5. It was found that a portion of the membrane and catalyst layer exhibited buckling distortion. MEA buckles under swelling [16]. This deformation is an initial mechanical degradation

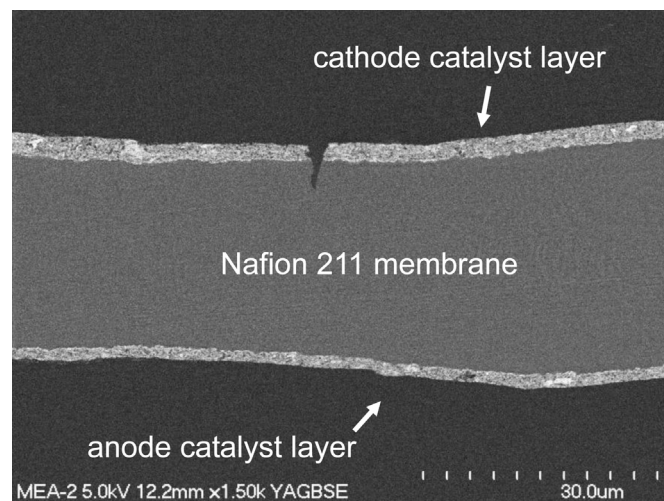Fig. 4. Humidity cycle test results.

Fig. 6. Cross-sectional SEM images of the MEA crack in the upper part of the cell after the humidity cycle tests (anode/cathode catalyst layer thickness: 2/2 μm).
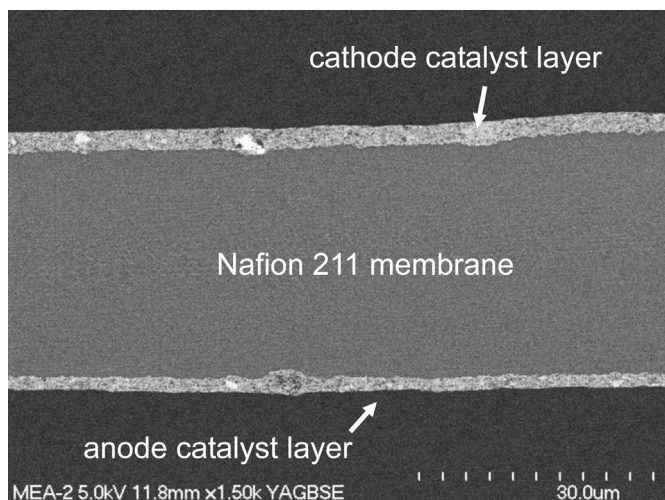
Fig. 7. Cross-sectional SEM images of the MEA in the lower part of the cell after the humidity cycle tests (anode/cathode catalyst layer thickness: 2/2 μm).

of the MEA causing locally large plastic strain. Fig. 6 shows cross-sectional SEM images of the same MEA from another view point in the upper part of the cell. As shown in the figure, a crack has formed from the catalyst layer to the membrane. The PEM was subjected to tensile stress under the catalyst layer crack [18,19] when the PEM was dehydrated. By repeating humidity cycles, cracks cause the formation of pinholes in the PEM. Preventing the MEA from buckling is an effective mitigation method used to suppress MEA mechanical degradation [16]. In cross-sectional SEM images of the MEA in the lower part of the cell (Fig. 7), buckling distortion or cracking was not observed. Since the upper part of the cell on the cathode side is close to the feed gas inlet, swelling–shrinking deformation could easily occur as a result of a change in the dew point of the supply gas. On the other hand, since liquid water could easily move to the lower part of the cell under the influence of gravity, the possibility of little change in humidity, such as near the gas outlet of the lower part of the cell, should be considered. Fig. 8 shows the cross-sectional SEM images of the MEA in the upper part of the cell after the humidity cycle tests. The thickness of both the anode and cathode catalyst layers was set at
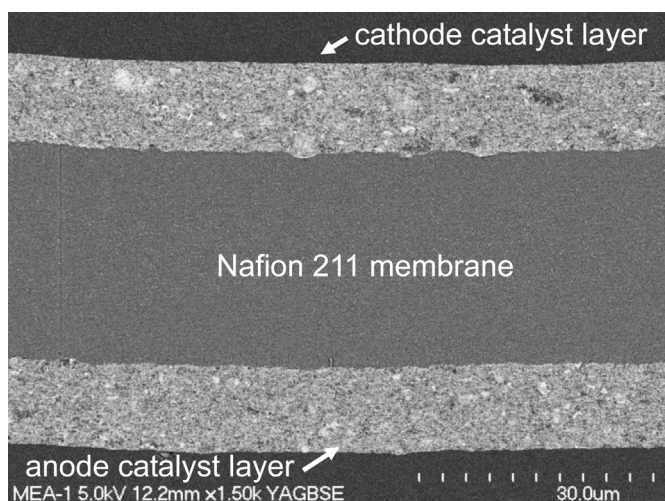

Fig. 8. Cross-sectional SEM images of the MEA in the upper part of the cell after the humidity cycle tests (anode/cathode catalyst layer thickness: 10/10 μm).

10 μm. The structure at the initial state was almost held and structural change in the MEA after the humidity cycle tests was not clearly observed in the SEM image of the observation position. A clear structural change or damaged spot could not be found in the SEM image obtained this time. However, when the thickness of a catalyst layer was large, it was found that there is a tendency for a membranous structural change to become small.

Based on the results of the humidity cycle tests and subsequent SEM observation of the two MEAs with different thickness of catalyst layers, it is considered that the thickness of catalyst layers of an MEA may have influenced the characteristics of structural change of MEA by humidity cycles. That is, the membranous mechanical deformation characteristics changed depending on the thickness of the catalyst layer of the MEA, and the mechanical strength was improved when the thickness of the catalyst layer was large.

4. Conclusions

The influence of the thickness of the catalyst layer of an MEA on the structural change of a polymer electrolyte membrane under humidity cycle tests was investigated. It was found that the catalyst layer thickness had no effect on the thermal deformation behavior of the membrane and MEA. However, the catalyst layer was found to reduce the dimensional change in the membrane as the thickness of the catalyst layer became larger from the SEM images obtained in this study. From the previous analysis of membrane wrinkle deformation, it was reported that a thicker membrane prevents buckling [16]. It is shown that increasing the thickness of a catalyst layer might result in similar effects as with increasing the membrane thickness. To improve the mechanical durability of the membrane evaluated by the humidity cycle tests, it is necessary to control the in-plane dimensional change of the membrane as reported previously. Comparing the mechanical durability of membranes by conducting humidity cycle tests, it is necessary to adjust the MEA specifications, especially the catalyst layer thickness.

References

[1] A. Iiyama, S. Iguchi, A. Daimaru, K. Shinohara, Objectives, R&D Challenge Topics and Proposed Evaluation Methods for Polymer Electrolyte Fuel Cells, FCCJ, 2007.
[2] A. Iiyama, K. Shinohara, A. Ohma, T. Yoshida, A. Daimaru, Objectives, R&D Challenge Topics and Proposed Evaluation Methods for Polymer Electrolyte Fuel Cells, FCCJ, 2011.
[3] Website of the Fuel Cell Commercialization Conference of Japan (FCCJ), 2007 (in Japanese), http://fccj.jp/pdf/19_01_kt.pdf.
[4] Website of the Fuel Cell Commercialization Conference of Japan (FCCJ), 2011 (in Japanese), http://fccj.jp/pdf/23_01_kt.pdf.
[5] A. Ohma, K. Shinohara, A. Iiyama, T. Yoshida, A. Daimaru, ECS Trans. 41 (1) (2011) 775.
[6] Y. Hashimasa, T. Numata, K. Moriya, S. Watanabe, J. Power Sources 155 (2) (2006) 182–189.
[7] Y. Hashimasa, T. Shimizu, Y. Matsuda, D. Imamura, M. Akai, ECS Trans. 50 (2) (2012) 723–732.
[8] A. Kusoglu, A.M. Karlsson, M.H. Santare, S. Cleghorn, W.B. Johnson, J. Power Sources 161 (2006) 987–996.
[9] A. Kusoglu, A.M. Karlsson, M.H. Santare, S. Cleghorn, W.B. Johnson, J. Power Sources 170 (2007) 345–358.
[10] A. Kusoglu, A.M. Karlsson, M.H. Santare, S. Cleghorn, W.B. Johnson, J. Electrochem. Soc. 157 (2010) B705–B713.

[11] M.N. Silberstein, M.C. Boyce, J. Power Sources 196 (2011) 3452–3460.
[12] T.T. Aindow, J. O'Neill, J. Power Sources 196 (2011) 3851–3854.
[13] Y.-H. Lai, Y. Li, J.A. Rock, J. Power Sources 195 (2010) 3215–3223.
[14] F.E. Hizir, S.O. Ural, E.C. Kumbur, M.M. Mench, J. Power Sources 195 (2010) 3463–3471.
[15] M.F. Serincan, U. Pasaogullari, J. Power Sources 196 (2011) 1303–1313.
[16] T. Uchiyama, M. Kato, T. Yoshida, J. Power Sources 206 (2012) 37–46.
[17] S. Kreitmeier, G.A. Schuler, A. Wokaun, F.N. Büchi, J. Power Sources 212 (2012) 139–147.
[18] Y.-H. Lai, D.A. Dillard, in: W. Vielstich, H.A. Gasteiger, H.H. Yokokawa (Eds.), Handbook of Fuel Cells, Advances in Electrocatalysis, Materials, Diagnostics and Durability, vol. 5, John Wiley & Sons, Ltd, 2009, pp. 403–419.
[19] S.F. Burlatsky, M. Gummalla, J. O'Neill, V.V. Atrazhev, A.N. Varyukhin, D.V. Dmitriev, N.S. Erikhman, J. Power Sources 215 (2012) 135–144.